Journal of Immunological Methods 365 (2011) 50–57

Contents lists available at ScienceDirect

Journal of Immunological Methods

journal homepage: www.elsevier.com/locate/jim

Research paper

Label-free assessment of high-affinity antibody–antigen binding constants. Comparison of bioassay, SPR, and PEIA-ellipsometry

Theo Rispens [a,*], Henk te Velthuis [a,b], Piet Hemker [c], Han Speijer [d], Wim Hermens [e], Lucien Aarden [a]

[a] Department of Immunopathology, Sanquin Research, Plesmanlaan 125, 1066 CX Amsterdam, The Netherlands
[b] Business Unit Reagents, Sanquin, Plesmanlaan 125, 1066 CX Amsterdam, The Netherlands
[c] CWI, Amsterdam and Korteweg-de Vries Institute, University of Amsterdam, Science Park 904, 1098 XH Amsterdam, The Netherlands
[d] Delbia B.V., Biopartner Center, Oxfordlaan 70, 6229 EV Maastricht, The Netherlands
[e] Maastricht University, Oxfordlaan 70, 6229 EV Maastricht, The Netherlands

ARTICLE INFO

Article history:
Received 20 April 2010
Received in revised form 30 September 2010
Accepted 19 November 2010
Available online 27 November 2010

Keywords:
High-affinity antibodies
PEIA-ellipsometry
Biacore

ABSTRACT

Assessment of high-affinity antibody–antigen binding parameters is important in such diverse areas as selection of therapeutic antibodies, detection of unwanted hormones in cattle and sensitive immunoassays in clinical chemistry. Label-free assessment of binding affinities is often carried out by immobilization of one of the binding partners on a biosensor chip, followed by monitoring the binding equilibrium of the other partner. However, for the measurement of high-affinity binding, with dissociation constants in the picomolar range or lower, equilibration times exceed practical limits and one has to resort to the measurement of sorption kinetics. Here we evaluate a new technique, using PEIA[1]-ellipsometry and establishment of equilibrium in solution. Binding parameters are determined for two high-affinity anti-interleukin 6 antibodies, anti-IL6.16 and anti-IL6.8, and compared with values obtained by a bioassay, based on IL6-dependent cell growth, and with values obtained by a standard technique based on SPR.[2] The high affinities of both antibodies as found with the bioassay (5 and 50 pM for anti-IL6.8 and anti-IL6.16, respectively), could be conveniently measured by PEIA-ellipsometry. Using SPR, equilibrium measurements indeed proved too time-consuming and analysis of adsorption/desorption kinetics revealed that the binding of the antibodies on the chip caused the appearance of different populations of antibodies with different affinities.

1. Introduction

Antibody–antigen binding is often measured by monitoring the adsorption of the antigen on a solid surface covered with the antibody. Such measurements are performed with various techniques, such as ellipsometry (Rothen, 1947), surface plasmon resonance (Fägerstam et al., 1992), quartz-crystal microbalance (Kösslinger et al., 1995) and interferometry (Piehler et al., 1997; Abdiche et al., 2008). For these so-called solid-phase techniques two different approaches are used. The equilibrium (dissociation) constant K_d is often obtained from *equilibrium experiments* and the binding rate constants k_{on} and k_{off}, and thus $K_d = k_{off}/k_{on}$, are obtained from *kinetic experiments*. As shown in the present study, both methods may run into problems for high-affinity binding.

PEIA-ellipsometry is a new method that takes advantage of the fact that establishment of binding equilibrium in solution is much faster than at a solid surface. The concentrations of unbound antigen in the solution are measured from the antigen adsorption on a slide covered with a small spot of antibody. For low protein concentrations such adsorption is limited but can be measured down to the femtomolar range by precipitation-enhancement (Speijer et al., 2004).

Here, we demonstrate this method to determine the binding parameters of two high-affinity anti-interleukin 6

* Corresponding author. Tel.: +31 20 512 3170; fax: +31 20 512 3171.
E-mail addresses: t.rispens@sanquin.nl (T. Rispens), h.tevelthuis@sanquin.nl (H. te Velthuis), p.w.hemker@cwi.nl (P. Hemker), h.speijer@delbia.nl (H. Speijer), w.hermens@maastrichtuniversity.nl (W. Hermens), l.aarden@sanquin.nl (L. Aarden).

[1] PEIA = Precipitate-Enhanced ImmunoAssay.
[2] SPR = Surface Plasmon Resonance.

0022-1759/$ – see front matter © 2010 Elsevier B.V. All rights reserved.
doi:10.1016/j.jim.2010.11.010

(IL6) antibodies, anti-IL6.16 and anti-IL6.8. K_d values were first measured with a bioassay, based on IL6-dependent cell growth, and were both found to be in the picomolar range. These values were then compared with the values obtained with PEIA-ellipsometry and with a standard SPR-based technique (Biacore).

2. Methods

2.1. Materials

Recombinant human IL6 was produced at Sanquin in Pichia pastoris and purified to apparent homogeneity by affinity chromatography on an anti-IL6.16 affinity column. IL6 concentrations were obtained by dilution of a stock solution (260 μg/ml). Concentration of the stock solution was determined by UV absorbance at 280 nm. Anti-IL6.16 and anti-IL6.8 antibodies (Sanquin) have been described before (Brakenhoff et al., 1990). Human transferrin was obtained from Sigma-Aldrich (St. Louis, USA). Buffers were prepared with de-ionized water (Milli-Q3 system, Millipore, Etten Leur, The Netherlands). Unspecific binding was suppressed with non-fat dry milk (NFDM) (Vremini Excellent, Vreugdenhil BV, Voorthuizen, The Netherlands) or with Tween 20 (Biorad, Veenendaal, The Netherlands). Silicon slides for ellipsometry and precipitation buffer for horseradish peroxidase (HRP)-labeled conjugates, used in the PEIA-ellipsometry experiments, were from Delbia B.V., Maastricht, The Netherlands.

2.2. Bioassay

The bioassay for IL6 was carried out as described (Aarden et al., 1987). In short, IL6-dependent murine B cell hybridomas (B9 cells) were cultured in Iscove's modified Dulbecco's medium (Biowhittaker, Basel, Zwitserland), containing 8 pg/ml human IL6, 5% fetal calf serum (Bodinco, Alkmaar, The Netherlands), 50 μM 2-mercaptoethanol, penicillin and streptomycin. Batches of 5000 of these cells were cultured at various IL6 concentrations in a final volume of 200 μL in flat-bottom microtitre plates. After 68 h, the cells were labeled with 0.2 μCi [^{3}H]thymidin (2 Ci/mmol) (Amersham, Houten, The Netherlands) and incorporated radioactivity was measured after 72 h by scintillation counting.

2.3. PEIA-ellipsometry

Ellipsometry was performed at room temperature with a new type of ellipsometer (Delbia B.V., Maastricht, The Netherlands) with 8 cuvettes equipped with magnetic stirrers (Damen et al., 2009). This optical technique allows real-time assessment of the surface mass $\Gamma(t)$ of protein on a reflecting slide from the changes in the positions of two polarizer prisms, the polarizer P and the analyzer A. Its sensitivity has been much improved by the adsorption of an HRP-labeled antibody to the adsorbed protein and HRP-catalyzed formation of precipitate (PEIA technique) (Speijer et al., 2004; Damen et al., 2009).

2.3.1. Coating of slides

Delbia slides type NW1 were coated with a small spot (7 mm^2) of anti-IL6.16 by application of a drop of 20 μg/mL antibody in 50 mM Tris buffer, pH 7.5, with 100 mM NaCl to the slide and incubation for 2 h at room temperature in a moist chamber. For anti-IL6.8, a drop of 50 μg/mL was incubated for 1 h in 10 mM bicarbonate buffer, pH 9.5, with 4.3 M NaCl. Slides were then flushed with Tris buffer with 1 mg/ml NFDM.

2.3.2. Equilibrium measurements

K_d values were determined by 3 h incubations of 0.68 pM IL6 with 0–160 pM anti-IL6.16, and overnight incubations of 1.06 pM IL6 with 0–15 pM anti-IL6.8, both in Tris buffer (50 mM, pH 7.5) containing 100 mM NaCl and 1 mg/mL NFDM.

The concentrations of unbound IL6 in the IL6/anti-IL6.16 mixtures were measured by inserting anti-IL6.16-coated slides for 10 min into the stirred mixtures, followed by washing (with Tris buffer) and incubation of the slides for 5 min in 1 μg/mL of anti-IL6.8/biotin conjugate (Sanquin). Slides were washed again, and incubated for 10 min in 1 μg/mL streptavidin-Poly HRP (Sanquin). For anti-IL6.8, the same procedure was used, except for incubation for 30 min in 50× diluted biotinylated polyclonal anti-IL6 antibody (Sanquin). Slides were then washed again and inserted in ellipsometer cuvettes filled with unstirred precipitation buffer and precipitate formation on the slides was measured and converted to free IL6 concentrations by means of a calibration curve (see Results). Note that the slides were coated with the same antibody as in the mixture because, besides free IL6, the IL6/antibody complexes could also adsorb when a different antibody was used. Measurements were performed in duplicate and K_d values were obtained by simultaneous fitting of the data to Eq. (6), using the Solver routine of Microsoft Excel.

2.3.3. Kinetic measurements

To measure the rate of association of IL6 and anti-IL6.16, 4 pM IL6 and 30 pM anti-IL6.16 were mixed at time $t = 0$, and the decreasing concentrations of free IL6 were measured at various time points by 5 min incubations of anti-IL6.16-covered slides, as described. To measure the rate of dissociation of IL6/anti-IL6.16 complexes, 400 pM IL6 was first incubated for 1 h with 1 nM anti-IL6.16 to reach equilibrium. At time $t = 0$, the mixture was then diluted 100 times and the increasing IL6 concentrations in the diluted mixture were measured. For anti-IL6.8 this procedure was repeated with 3 pM IL6 and 3 pM anti-IL6.8 for the association experiment. For the dissociation experiment, 150 pM of IL6 and 150 pM of anti-IL6.8 were incubated for 1 h and then diluted 50 times at time $t = 0$. Association and dissociation curves were measured in duplicate and used simultaneously for parameter fitting. Such fitting, and estimation of error indicated as ±SD or as 95% confidence limits, was performed with the Mathematica 7 program (Wolfram Research), using computational methods and statistics as described (Stortelder, 1998).

2.4. Surface plasmon resonance (SPR)

SPR measurements were performed with a Biacore 3000 system (Biacore AB, Breda, The Netherlands) at 25 °C. The instrument has a maximal sample volume of 250 μL and is equipped with 4 flow cells that can be used in series. Anti-IL6.16 and anti-IL6.8 were bound covalently to CM5 sensor chips at a concentration of 5 μg/mL in 10 mM sodium acetate pH 4.5,

using *N*-hydroxysuccinimide/1-ethyl-3-(3-dimethylaminopropyl) carbodiimide hydrochloride. Similarly, transferrin, with an isoelectric point close to that of IgG, was coupled as negative control, that is, adsorptions obtained in this cell were subtracted from the adsorptions in the other cells. Biacore buffer, i.e. 10 mM HEPES, pH 7.4, containing 3.4 mM EDTA, 0.15 mM NaCl, and 0.005% Tween 20, with various concentrations of IL6 was then passed through the cells at a flow rates of 1, 5, 10 or 30 μL/min, and the surface mass Γ(t) of adsorbed IL6 on the chip was measured real time and expressed in Resonance Units (RU). After each run, bound IL6 was removed in a regeneration step by injecting 5 μL of 0.1 M H_3PO_4 at 20 μL/min. Experiments were performed for 4 different IL6 concentrations and parameter fitting was performed as described in Section 2.3.3.

2.5. Data analysis

2.5.1. Complex formation in solution

For the formation of a complex C(t) of two binding partners A(t) and B(t) we have:

$$A(t) + B(t) \underset{k_{off}}{\overset{k_{on}}{\rightleftharpoons}} C(t) \quad \text{with } dC(t)/dt = k_{on}A(t)B(t) - k_{off}C(t) \tag{1}$$

with t for time and k_{on}, k_{off} the rate constants for association and dissociation of complex C.

The concentration of complexes at time t, is then given by the solution of Eq. (1):

$$C(t) = K_1(1 + f(t)) / (1 - f(t)) + K_2 \tag{2}$$

with $f(t) = [(C_0 - K_1 - K_2)/(C_0 - K_2 + K_1)]\ \exp(2K_1 k_{on} t)$, $K_1 = ½\sqrt{((A_{tot} + B_{tot} + K_d)^2 - 4A_{tot}\ B_{tot})}$, $K_2 = ½(A_{tot} + B_{tot} + K_d)$, and A_{tot} and B_{tot} the total concentrations of A and B . In association experiments we have $C_0 = 0$, and in dissociation experiments C_0 equals the initial concentration of complexes.

2.5.2. Complex formation on a chip surface

For complex formation on a surface, three different situations may exist (Hermens et al., 2004). For low-affinity binding, that is, for low k_{on} values, one remains in the so-called "kinetic" range, without significant concentration gradients of adsorbent at the surface. In that case, one may substitute a fixed buffer concentration A_b for A(t) in Eq. (1) and one finds:

$$\Gamma(t) = [1 - exp(-k_{on}(K_d + A_b)t)][\Gamma_{max}A_b / (K_d + A_b)], \tag{3}$$

where the surface concentration of complexes has been written as Γ(t) and the total surface concentration B_{tot} has been written as the maximal binding capacity Γ_{max}.

For higher k_{on} values one enters in the so-called "intermediate"range with depletion of adsorbent in the surface boundary layer. Adsorption rates will then be influenced by transport conditions, that is, by diffusion and flow rates. The same is true for desorption rates, because molecules desorbing from the surface are likely to re-adsorb and net desorption will be slow. As a result, one obtains apparent sorption constants $k_{on,app}$ and $k_{off,app}$ that underestimate the true k_{on} and k_{off} values (Corsel et al., 1986; Gemmell et al., 1988; Andree et al., 1994) and adsorption can be described by (Corsel et al., 1986):

$$d\Gamma(t)/dt = k_{on,app}A_b(\Gamma_{max} - \Gamma(t)) - k_{off,app}\Gamma(t), \tag{4}$$

with $k_{on,app} = k_{on}/(1 + (d/D)k_{on}(\Gamma_{max} - \Gamma))$, $k_{off,app} = k_{off}/(1 + (d/D)k_{on}(\Gamma_{max} - \Gamma))$, d the thickness of the boundary layer, D the diffusion constant of the adsorbent, Γ_{max} the maximal binding capacity and A_b the bulk concentration of the adsorbent in solution.

For even higher k_{on} values one enters into the so-called "transport-limited" range. The concentration of adsorbent directly at the surface will now be close to zero and k_{on} or k_{off} cannot be obtained from sorption kinetics because these are completely determined by the transport conditions of the system and the buffer concentration A_b. In that case we have for an SPR flow cell (Corsel et al., 1986, Hermens et al., 2004):

$$(d\Gamma/dt)_{intial} = (D/d)A_b = 0.49\, D^{2/3}Q^{1/3}(H/2)^{-2/3}(W/2)^{-1/3}x^{-1/3}A_b, \tag{5}$$

with Q the volume flow, H and W the height and width of the flow cell, and x the downstream distance from the edge of the adsorbing chip surface. Writing this relation as $d/D = 1/[D^{2/3}Q^{1/3}(H/2)^{-2/3}(W/2)^{\ -1/3} \times^{-1/3}]$ and inserting the values of $D = 9.0 \times 10^{-7}$ $cm^2 s^{-1}$ (DiLeo et al., 2009), $H/2 = 0.001$ cm, $W/2 = 0.025$ cm, $x = 0.12$ cm, and $Q = 8.33 \times 10^{-5}$ mL s^{-1} (= 5 μL/min) we find $d/D = 7.2 \times 10^2$ cm^{-1} s. For a flow rate of 10 μL/min we find $d/D = 6.4 \times 10^2$ cm^{-1} s.

2.5.3. Estimation of K_d values from equilibrium measurements

For equilibrium in solution, Eq. (1) reduces to $k_{on}A_{eq}B_{eq} = k_{off}C_{eq}$. Writing $Kd = k_{off}/k_{on}$ and $B_{tot} - C_{eq}$ for B_{eq}, we obtain the well-known Langmuir-equation:

$$C_{eq} = B_{tot}A_{eq} / \left(K_d + A_{eq}\right) \tag{6}$$

K_d values were obtained by fitting Eq. (6) to a series of A_{eq}, C_{eq} values. Note that this will only work for A_{eq} values not much larger than K_d because that would make Eq. (6) insensitive to K_d.

2.5.4. Estimation of k_{on}, k_{off}, K_d values from complex formation kinetics

For the PEIA experiments in solution, the rate constants k_{on} and k_{off} (and thus $K_d = k_{off}/k_{on}$) were obtained by fitting the data to Eq. (2). For the SPR experiments on a chip these parameters were obtained by fitting the data to Γ(t) as obtained from numerical integration of Eq. (4).

2.5.5. Verification of transport limitation

After an initial rapid phase, adsorption rates in the SPR experiments leveled-off (Fig. 7), indicating that they could no longer be transport-limited. To investigate a possible transport limitation in the initial phase, additional experiments with flow rates of 10 and 30 μL/min were performed. To exclude any inaccuracies because of dilution error in A_b we did not compare initial adsorption rates between separate

experiments, but between two cells in series, both containing chips coated with anti-IL6.8.

Integration of Eq. (5) over the whole chip, that is x = 0 to L cm, yields $d\Gamma_{tot}/dt = 0.74D^{2/3}Q^{1/3}(H/2)^{-2/3}(W/2)^{-1/3}L^{2/3}A_b$ for the total adsorption per second of IL6 in the cell. The total amount of IL6 passing through the cell per second equals $Q \cdot A_b$, so the fractional depletion of IL6 due to its passage through the cell is given by:

$$\text{fractional depletion} = 0.74D^{-2/3}Q^{-2/3}(H/2)^{-2/3}(W/2)^{1/3}L^{2/3}. \quad (7)$$

Note that depletion is independent of A_b and will become less for higher flow rates Q.

3. Results

3.1. Time-to-equilibrium in solution and at the biochip surface

The formation of antibody/antigen complexes was calculated for three different binding affinities: a hypothetical antibody with low binding affinity ($k_{on} = 10^3\ M^{-1}\ s^{-1}$, $k_{off} = 10^{-3}\ s^{-1}$, $K_d = 10^{-6}$ M), a hypothetical antibody with intermediate binding affinity ($k_{on} = 5\times10^5\ M^{-1}\ s^{-1}$, $k_{off} = 5\times10^{-4}\ s^{-1}$, $K_d = 10^{-9}$ M) and a high-affinity antibody with the binding parameters of anti-IL6.8, as presented in Table 1 ($k_{on} = 10^7\ M^{-1}\ s^{-1}$, $k_{off} = 5\times10^{-5}\ s^{-1}$, $K_d = 5\times10^{-12}$ M). To be able to extract K_d values from these data, antigen concentrations should not be much higher than K_d (see Section 2.5.3), so the antigen concentrations were taken as twice the K_d values. Calculations were performed for binding in solution, using Eq. (2), and for binding on a biochip surface, using Eq. (3) for the low-affinity case and numerical integration of Eq. (4) for the intermediate and high-affinity cases.

Results are shown in Fig. 1, showing that equilibration in solution is established much faster than at the chip surface. Even in solution, however, high-affinity equilibration takes several hours, which prompted us to use overnight incubation of anti-IL6.8 and IL6. Studying this equilibration at the chip surface is not feasible as shown by the fact that, even after 10 h, surface binding did not reach 20% of its equilibrium value.

Table 2
Ratios of the adsorption rates on two chips in series, both coated with anti-IL6.8.

IL6 concentration (nM)	Flow rate (μL/min)	Observed adsorption rate ratio cell 2/cell 1	Theoretical transport-limited rate ratio
12.7	5	0.75	0.76
12.7	5	0.73	0.76
6.4	5	0.76	0.76
3.2	5	0.65	0.76
1.6	5	0.65	0.76
12.7	10	0.71	0.85
12.7	10	0.67	0.85
6.4	10	0.68	0.85
3.2	10	0.65	0.85
1.6	10	0.65	0.85
12.7	30	0.62	0.93

3.2. Bioassay

IL6-dependent growth of B9 cells is shown in Fig. 2. Addition of anti-IL6 reduced the free concentration of IL6 and growth rate. Dissociation constants can be calculated from these data. As an example, if it is assumed that similar growth rates (cpm) correspond to similar IL6 concentrations it follows from Fig. 2 that, due to the presence of 10 ng/mL (66.7 pM) of anti-IL6.8, the total IL6 concentration of 31 pg/mL (1.32 pM) corresponded to the (interpolated) value of 2.56 pg/mL (0.11 pM) of free IL6. Assuming 2 binding sites per antibody molecule, we had 133 pM of IL6 binding sites, and we obtain from Eq. (6):

$$K_d = [anti-il6.8]_{free} / [IL6]_{free}/[IL6]_{bound}$$
$$= (133-(1.32-0.11)(0.11)/(1.32-0.11)) = 12\,\text{pM}.$$

This analysis results in average dissociation constants of 10 ± 2 pM and 107 ± 10 pM for anti-IL6.8 and anti-IL6.16, respectively. True K_d values will be lower because of consumption of IL6 from the culture medium by the B9 cells during the incubation period before label was added. In separate experiments this consumption was estimated to be 30–60% (Aarden et al., 1985), resulting in values of ca. 4–7 pM for anti-IL6.8 and 40–70 pM for anti-IL6.16, respectively (Table 1).

Table 1
Binding parameters for binding of IL6 to anti-IL6.16 and to anti-IL6.8.

		Bioassay	PEIA	SPR
Equilibrium measurements				
Anti-IL6.16	K_d (pM)	40–70	47 ± 10	<400
Anti-IL6.8	K_d (pM)	4–7	3.7 ± 0.8	<200
Kinetic measurements				
Anti-IL6.16	K_d (pM)	–	51 (40–62)	Multiple populations of binding sites (see text).
	$k_{on}(M^{-1}\,s^{-1})$	–	$3.0\ (2.3–4.1)\times10^6$	
	$k_{off}\ (s^{-1})$	–	$1.5\ (1.1–2.1)\times10^{-4}$	
Anti-IL6.8	K_d (pM)	–	6.2(4.5–7.1)	Multiple populations of binding sites (see text).
	$k_{on}\ (M^{-1}\,s^{-1})$	–	$9.0(6.3–12)\times10^6$	
	$k_{off}\ (s^{-1})$	–	$0.6(0.3–0.8)\times10^{-4}$	

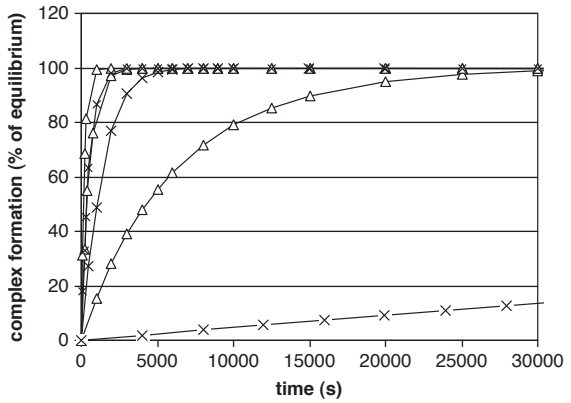

Fig. 1. Approach to equilibrium for complex formation in solution (Δ) and at a chip surface (x). In both cases, the upper curve is for low-affinity, the middle curve is for intermediate affinity and the lower curve is for high affinity (see text).

3.3. PEIA-ellipsometry

3.3.1. Equilibrium measurements

Fig. 3 shows the dose–response curve used to determine (free) IL6 concentrations from the initial rates of change of the polarizer P due to precipitate formation, using anti-IL6.16-coated slides. For a range of IL6 concentrations, initial rates of change were calculated as the derivative at t = 0 of a 2nd order polynomial that was fitted through the first 4 data points of each curve (upper panel). The lower panel shows the resulting dose-response curve. A 2nd order polynomial was fitted through these points and used as calibration curve to determine free IL6 concentrations in subsequent experiments.

To obtain K_d values from equilibrium in solution, IL6 was incubated with several concentrations of anti-IL6.16 for 3 h or anti-IL6.8 overnight, allowing equilibrium to be established, and concentrations of free IL6 were determined, as shown in Fig. 4. Assuming 2 binding sites per anti-IL6 molecule, K_d values were obtained from these data as described, and were in good agreement with the values obtained from the bioassay (Table 1).

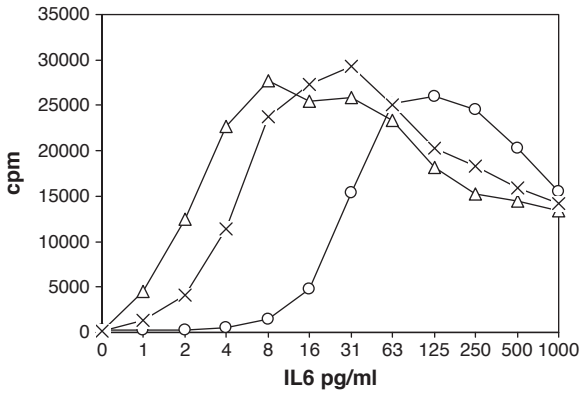

Fig. 2. Effects of IL6 concentrations on cell growth, expressed as the counts per minute (cpm) of incorporated ^{3}H-thymidine (Δ). Values obtained after addition of 10 ng/mL anti-IL6.8 or 10 ng/mL anti-IL6.16 are indicated by (o) and (X), respectively.

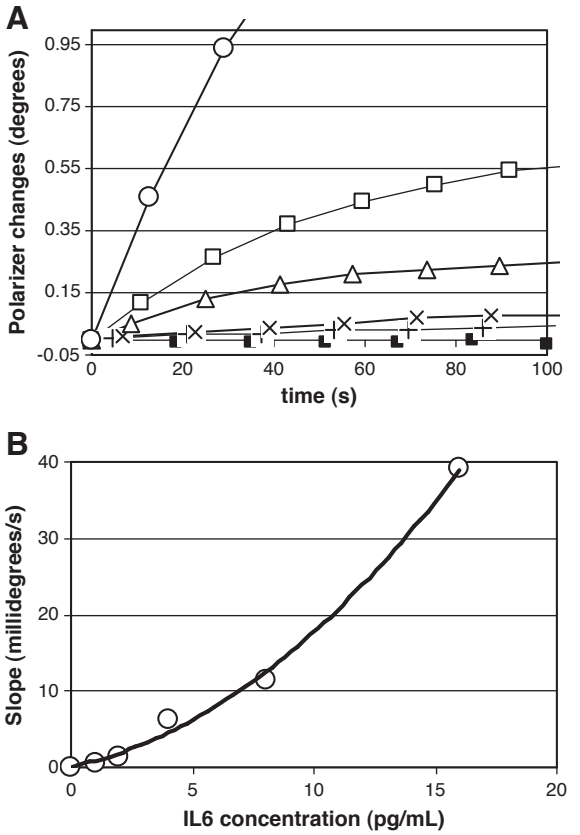

Fig. 3. Determination of free IL6 concentrations with the PEIA technique for anti-IL6.16-coated slides. The upper figure shows polarizer changes for IL6 concentrations of 0(■), 1(+), 2(x), 4(Δ), 8(□) and 16(o) pg/ml. The lower figure shows the initial rates of polarizer changes thus obtained, that is, 0.03, 0.7, 1.3, 6.2, 11.5 and 39.1 millidegrees per second.

3.3.2. Kinetic measurements

Association rates were determined by measuring free IL6 at various time-points after mixing IL6 with anti-IL6.16 or anti-IL6.8. Similarly, dissociation rates were obtained by measuring free IL6 after diluting pre-formed IL6/anti-IL6 complexes (Fig. 5). Simultaneous fits of Eq. (2) to association and dissociation data are shown in Fig. 5 and the obtained parameter values are given in Table 1 . The dissociation constants calculated from the kinetic constants agree with those obtained from equilibrium measurements. The higher affinity of anti-IL6.8 compared to anti-IL6.16 appears to be due to a combination of both a higher on-rate and a smaller off-rate.

3.4. SPR experiments

3.4.1. Initial transport limitation of SPR adsorption curves

Using two cells in series, the depletion of Il6 in the first cell will lower the adsorption rate in the second cell. Using Eq. (7) for transport-limited flow one finds that for flow rates of 5, 10 and 30 μL/min depletion will be 24%, 15% and 7%, respectively. To improve differentiation between transport-limited and intermediate range adsorption, the first chip was coated with 1400 RU and the second chip with 1000 RU of anti-IL6.8. For transport-limited adsorption this difference in Γ_{max} should have no effect, but in the intermediate range we find from

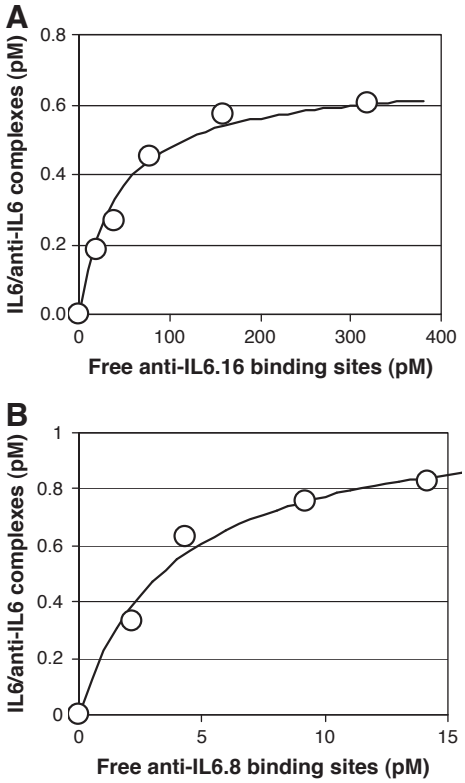

Fig. 4. Concentrations of IL6/anti-IL6 complexes as a function of the concentration of free binding sites. Best fitting theoretical curves with $K_d = 47$ pM for anti-IL6.16 (upper panel) and Kd = 3.7 pM for anti-IL6.8 are also shown.

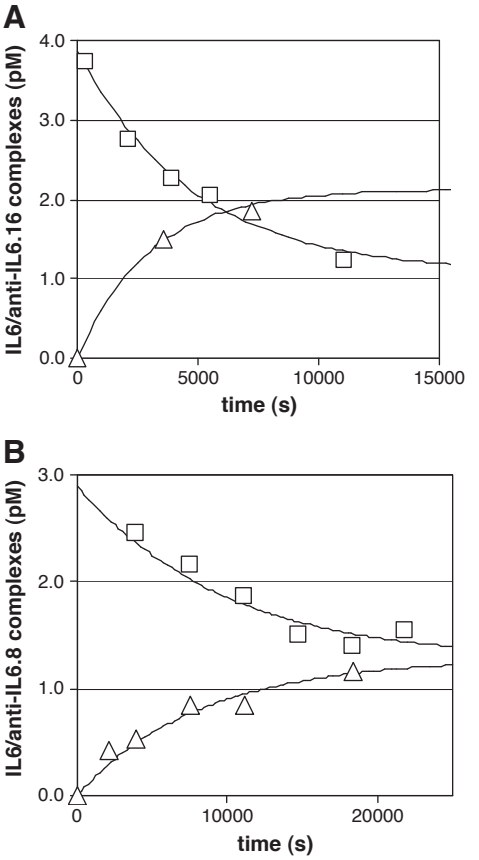

Fig. 5. Association (Δ) and dissociation (□) experiments for IL6/anti-IL6.16 complexes (upper figure) and IL6/anti-IL6.8 complexes (lower figure) with best-fitting curves. (See text).

Eq. (4) that the initial adsorption rate will approximately be equal to $k_{on,app}A_b\Gamma_{max}$ and, due to the lower Γ_{max} value in the 2nd cell, this rate would then be about 30% lower than in the first cell. Results of these experiments are shown in Table 2. For the experiments at 10 μL/min it can be immediately concluded that they are not transport-limited, because the slope ratio is much smaller than the corresponding value of 0.85. Apparently, the lower Γ_{max} in the 2nd cell now causes slower adsorption, as expected in the intermediate range. The same conclusion follows from the experiment at a flow rate of 30 μL/min, with the 38% reduction of the adsorption rate in the 2nd cell mainly caused by the 30% reduction of Γ_{max}. For the experiments at a flow rate of 5 μL/min, the high IL6 concentrations (12.7 and 6.4 nM) indeed approximately show the predicted 24% reduction of initial adsorption rates, indicating transport limitation. However, for both 5 and 10 μL/min, the lower IL6 concentrations in Table 2 show lower rate ratios. This could be related to a low-affinity population of binding sites (see later discussion) or to some aspecific IL6 adsorption, in addition to the adsorption on the chip, that would affect the lower concentrations most.

3.4.2. Equilibrium measurements

It was attempted to obtain K_d values using SPR by monitoring the establishment of equilibrium at various concentrations of IL6 on chips covered with either anti-IL6.16 or anti-IL6.8. On a Biacore system with 250 μL as a maximum injection volume and 1 μL/min as minimal flow speed, 4 h is the maximum time to monitor an undisturbed association curve. As seen in Fig. 6, at concentrations below ca. 1 nM, measurements lasting up to 4 h failed to reach equilibrium. Hence, no K_d values could be obtained. Nevertheless, maximal adsorptions of about 360 RU on anti-IL6.16 and 260 RU on anti-IL6.8 can be estimated (lower figure) and half-maximal values were exceeded for total IL6 concentrations of 400 pM and 200 pM of IL6, respectively. Because of the negligible amounts of adsorbed IL6 these values approximate the concentrations of free IL6 and it follows from Eq. (6) that average K_d values will be <400 pM for anti-IL6.16, and <200 pM for anti-IL6.8.

3.4.3. Kinetic measurements

Adsorption experiments were carried out on chips coated with either anti-IL6.16 or anti-IL6.8 with 12.7, 6.4, 3.2 and 1.6 nM of IL6 at a flow speed of 5 μL/min as shown in Fig. 7 for the highest and lowest IL6 concentrations. For anti-IL6.16, 50% desorption was observed after 3 h, whereas only about 10% desorption is observed for anti-IL6.8. These data, were fitted to Eq. (4) but produced unsatisfactory fits, especially for the high IL6 concentrations (Fig. 7).

Therefore, a model with two populations of binding sites was also fitted to the data, that is, $d\Gamma(t)/dt = d\Gamma_1(t)/dt + d\Gamma_2(t)/dt$ with the two terms on the right equal to expression (4). It was attempted to obtain the 6 parameters k_{on1}, K_{d1}, k_{on2},

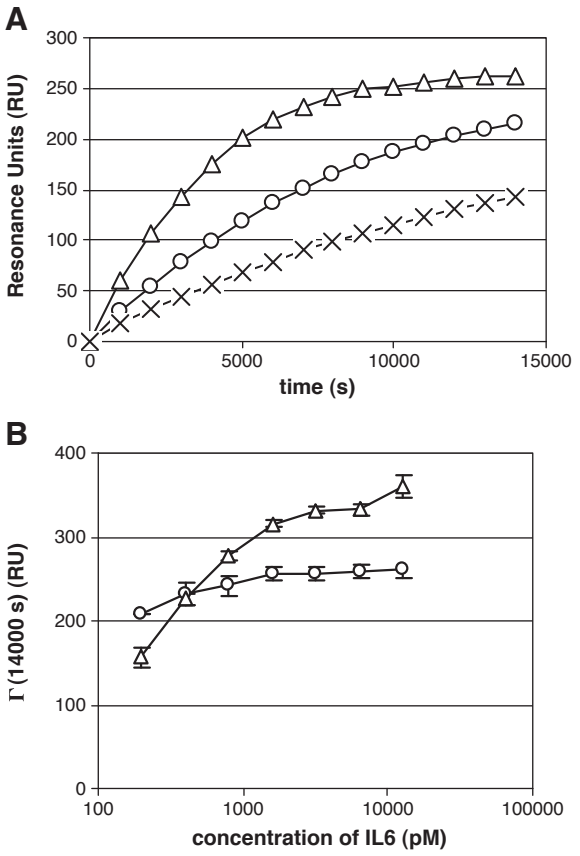

Fig. 6. Upper pane: Adsorptions of 0.8 (Δ), 0.4 (o) and 0.2 nM (X) IL6 on SPR chips covered with anti-IL6.16. Lower pane: Values of RU at t = 14,000 s for chips covered with anti-IL6.16 (Δ) or anti-IL6.8 (o).

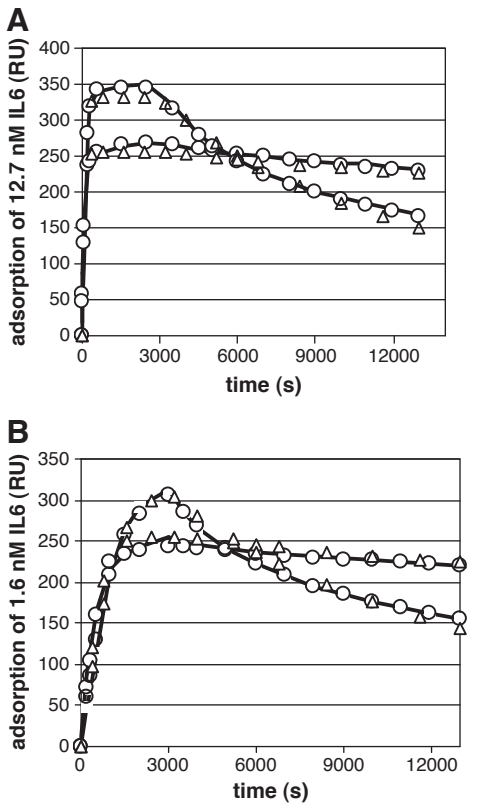

Fig. 7. Adsorptions of IL6 on anti-IL6.16 and anti-IL6.8, as measured by SPR. Measured data are indicated by drawn lines, with the curves reaching the highest values indicating the adsorptions on and upper and lower curves indicate adsorptions on anti-IL6.16 and anti-IL6.8, respectively. Best-fit results are indicated by (O) for a 2-population model and by (Δ) for a one-population model.

K_{d2}, Γ_{max1} and Γ_{max2} but the model only converged when the four curves with different IL6 concentrations were fitted simultaneously. In that case, obtained parameter values with 95% confidence limits, were:

High-affinity population of anti-IL6.16:

$$k_{on} = 0.8(0.7-1.0) \times 10^6 M^{-1}s^{-1}; K_d = 55(48-56)\ \text{pM}; \Gamma_{max} = 1.1(1.0-1.2)\text{pmol}\cdot\text{cm}^{-2}.$$

Low-affinity population of anti-IL6.16:

$$k_{on} = 1.1(0.5-1.2)\text{x}10^6\text{M}^{-1}\text{s}^{-1}; K_d = 500(400-1200)\text{pM}; \Gamma_{max} = 0.5(0.4-0.6)\text{pmol.cm}^{-2}.$$

High-affinity population of anti-IL6.8:

$$k_{on} = 3.8(3.7-4.1) \times 10^6 M^{-1}s^{-1}; K_d = 1.0(0.4-4.17)\text{pM}; \Gamma_{max} = 0.9(0.8-1.0)\text{pmol}\cdot\text{cm}^{-2}.$$

Low-affinity population of anti-IL6.8:

$$k_{on} = 1.6(1.5-4.1) \times 10^5 M^{-1}s^{-1}; K_d = 700(600-1100)pM; \Gamma_{max} = 0.2(0.1-0.3)\text{pmol}\cdot\text{cm}^{-2}.$$

It seemed that, for both anti-IL6 antibodies, adsorption on the chip caused the appearance of a second population of binding sites with much lower affinity. The fact that the 3-parameter model for only a single population of binding sites produced a better fit for the IL6 adsorption on anti-IL6.8 than on anti-IL6.16 (see Fig. 7) probably reflects the much smaller fraction of low-affinity binding sites found on chips coated with anti-IL6.8.

4. Discussion

The present study demonstrates that by using PEIA-ellipsometry, K_d values can be determined up to the low picomolar range and theoretically even for much higher affinity. Furthermore, it is shown that such K_d values may be estimated from equilibrium measurements as well as from k_{on} and k_{off} values as measured in kinetic experiments.

K_d measurement with PEIA-ellipsometry takes advantage of the relatively fast establishment of equilibrium in solution. By contrast, it can be understood from general principles that routine K_d measurement from equilibrium binding on biosensor chips will not be feasible for high-affinity binding. Even in effectively stirred fluids or rapidly perfused flow cells, the maximal, transport limited, rate constant for the adsorption of proteins with $M_w = 50–150$ kDa from solution onto a solid

surface will not exceed 0.003 cm s^{-1} (Corsel et al., 1986). Measurement of a K_d value of 1 pM from equilibrium implies using protein concentrations in that range, that is, 10^{-15} mol/cm^3, with a maximal adsorption rate of $0.003\times10^{-15}=3\times10^{-18}$ mol/cm^2/s. Minimal well-measurable equilibrium values of adsorbed proteins are in the range of 10 ng/cm^2 or 10^{-13} mol/cm^2 for a protein of 100 kDa. So this would take $10^{-13}/3\times10^{-18}=3.3\times10^4$ s = 9.2 h. In practice it would take even much longer because the adsorption rate will slow down when equilibrium is reached. Also, for high-affinity binding, the sorption rate constants k_{off} and k_{on} cannot be accurately determined from surface sorption kinetics because $k_{off,app}$ becomes too small to be accurately measured in a reasonable time.

Measurement of protein–protein binding at solid surfaces also entails the risk of influencing binding affinity by adsorption-induced changes in the binding partner on the surface. In the present study this is illustrated by the appearance of low-affinity populations of binding sites upon adsorption of anti-IL6.16 and anti-IL6.8 on the chip, and similar observations have been reported before (Svitel et al., 2007; Yeung and Leckband, 1997). To identify the relevant population one could try to switch free and bound partners, but the free antibody in solution may then bind with both binding sites to the antigen on the surface and thereby become almost irreversibly bound. In the present study desorption of antibody was indeed negligible after binding to chips coated with IL6 (results not shown). Alternatively, one could try to use more gentle procedures for the binding of antibody to the chip than the covalent coupling used in the present study, e.g. by using protein G-coated slides to capture the antibody.

In summary, we demonstrated that PEIA-ellipsometry is a useful technique to accurately determine binding constants for K_d values in the picomolar range.

References

Aarden, L., Lansdorp, P., De Groot, E., 1985. A growth factor for B cell hybridomas produced by human monocytes. Lymphokines 10, 175.

Aarden, L.A., De Groot, E.R., Schaap, O.L., Lansdorp, P.M., 1987. Production of hybridoma growth factor by human monocytes. Eur. J. Immunol. 17, 1411.

Abdiche, Y., Malashock, D., Pinkerton, A., Pons, J., 2008. Determining kinetics and affinities of protein interactions using a parallel real-time label-free biosensor, the Octet. Anal. Biochem. 377, 209.

Andree, H.A.M., Contino, P.B., Repke, D., Gentry, R., Nemerson, Y., 1994. Transport rate limited catalysis on macroscopic surfaces: The activation of factor X in a continuous flow enzyme reactor. Biochemistry 33, 4368.

Brakenhoff, J.P., Hart, M., De Groot, E.R., Di Padova, F., Aarden, L.A., 1990. Structure-function analysis of human IL-6. Epitope mapping neutralizing monoclonal antibodies with amino- and carboxyl-terminal deletion mutants. J. Immunol. 145, 561.

Corsel, J.W., Willems, G.M., Kop, J.M.M., Cuypers, P.A., Hermens, W.T., 1986. The role of intrinsic binding rate and transport rate in the adsorption of prothrombin, albumin and fibrinogen to phospholipid bilayers. J. Colloid Interface Sci. 111, 544.

Damen, C.W.N., Speijer, H., Hermens, W.T., Schellens, J.H.M., Rosing, H., Beijnen, J.H., 2009. The bioanalysis of trastuzumab in human serum using precipitate-enhanced ellipsometry. Anal. Biochem. 393, 73.

DiLeo, M.V., Kellum, J.A., Federspiel, W.J., 2009. A simple mathematical model of cytokine capture using a hemoadsorption device. Ann. Biomed. Eng. 37, 222.

Fägerstam, L.G., Frostell-Karlsson, A., Karlsson, R., Persson, B., Rönnberg, I., 1992. Biospecific interaction analysis using surface plasmon resonance detection applied to kinetic, binding site and concentration analysis. J. Chromatogr. 597, 397.

Gemmell, C.H., Turitto, V., Nemerson, Y., 1988. Flow as a regulator of the activation of factor X by tissue factor. Blood 72, 1404.

Hermens, W.T., Benes, M., Richter, R., Speijer, H., 2004. Effects of flow on solute exchange between fluids and supported biosurfaces. Biotechnol. Appl. Biochem. 39, 277.

Kösslinger, C., Uttenthaler, E., Drost, S., Aberl, F., Wolf, H., Brink, G., Sackmann, A., Stranglmaier, E., 1995. Comparison of the QCM and the SPR method for surface studies and immunological applications. Sens. Actuators B 24–25, 107.

Piehler, J., Brecht, A., Giersch, T., Hock, B., Gauglitz, G., 1997. Assessment of affinity constants by rapid solid phase detection of equilibrium binding in a flow system. J. Immunol. Meth. 201, 189.

Rothen, A., 1947. Immunological reactions between films of antigen and antibody molecules. J. Biol. Chem. 168, 75.

Speijer, H., Laterveer-Vreeswijk, R.H., Glatz, J.F.C., Nieuwenhuizen, W., Hermens, W.T., 2004. One-step immunoassay for measuring protein concentrations in plasma, based on precipitate-enhanced ellipsometry. Anal. Biochem. 326, 257.

Stortelder, W.J.H., 1998. Parameter estimation in nonlinear dynamic systems: CWI Tracts, 124, p. 1 (http://oai.cwi.nl/oai/asset/13145/13145A.pdf).

Svitel, J., Boukari, H., Van Ryk, D., Wilson, R.C., Schuck, P., 2007. Probing the functional heterogeneity of surface binding sites by analysis of experimental binding traces and the effect of mass transport limitation. Biophys. J. 92, 1742.

Yeung, C., Leckband, D.E., 1997. Molecular level characterization of micro-environmental influences on the properties of immobolized proteins. Langmuir 13, 6746.